NASA TN D-1828

TECHNICAL NOTE

D-1828

THEORETICAL INVESTIGATION OF THE SLIDEOUT DYNAMICS OF A VEHICLE EQUIPPED WITH A TRICYCLE SKID-TYPE LANDING-GEAR SYSTEM

By Richard B. Noll and Robert L. Halasey

Flight Research Center
Edwards, Calif.

NATIONAL AERONAUTICS AND SPACE ADMINISTRATION
WASHINGTON

May 1963

NATIONAL AERONAUTICS AND SPACE ADMINISTRATION

TECHNICAL NOTE D-1828

THEORETICAL INVESTIGATION OF THE SLIDEOUT DYNAMICS OF A VEHICLE EQUIPPED WITH A TRICYCLE SKID-TYPE LANDING-GEAR SYSTEM

By Richard B. Noll and Robert L. Halasey

SUMMARY

A theoretical analysis is presented for the slideout dynamics of a vehicle equipped with a tricycle skid-type landing-gear system. These equations are reduced to three degrees of freedom, and the results of numerical calculations are compared to flight-test data obtained from the X-15 research vehicle. A comparison of these results shows that the three-degree-of-freedom equations can be used to adequately predict the slideout distance, the direction of lateral displacement, and the approximate lateral displacement. A numerical study shows that the velocity at which the aerodynamic influence on the vehicle becomes negligible can be predicted by the three-degree-of-freedom equations.

INTRODUCTION

The successful recovery of a space vehicle is completed by a landing which assures the safety of the personnel and equipment onboard the vehicle. In addition to absorbing the impact loads, the landing system of the space vehicle which performs a horizontal landing must provide stability and controllability during the subsequent runout. These characteristics, which are obtained on most conventional aircraft by a landing-gear system utilizing a three-point arrangement and equipped with brakes and steerable wheels, have been extensively treated by many investigators (refs. 1 to 4, for example). The inherent stability of the tricycle landing-gear system and the extensive experience gained from use on conventional aircraft make this type of system attractive for space vehicles.

A tricycle system consisting of two main gear equipped with skids, placed symmetrically to the rear of the vehicle, and a nose gear, equipped with either a skid or a wheel, located on the forward section was studied in references 5 to 9 for use on space vehicles. Landing impact has been investigated both analytically (ref. 7) and experimentally (refs. 5, 6, 8, and 9). Slideout (runout) results obtained from flight and model tests (refs. 8 and 9) verify the directional stability of the skid-type tricycle system during slideout; however, these results pertain to a particular vehicle and landing-gear configuration and cannot be applied directly to the design of other space vehicles. In addition, these tests did not evaluate controllability during the slideout.

In order to provide a method for evaluating the slideout characteristics as well as the controllability of future vehicles, this paper presents a comprehensive theoretical investigation of the slideout dynamics of a vehicle equipped with a skid-type tricycle landing-gear system. Results of numerical calculations obtained on a digital computer are compared with flight-test results in order to assess the validity of the theoretical investigation.

SYMBOLS AND COEFFICIENTS

b wing span, ft

C_D drag coefficient, $\frac{\text{Drag}}{\bar{q}S}$

$C_{D_{\delta_h}}$ rate of change of drag coefficient with horizontal-tail deflection, $\frac{\partial C_D}{\partial \delta_h}$, per radian

C_L lift coefficient, $\frac{\text{Lift}}{\bar{q}S}$

$C_{L_{\delta_h}}$ rate of change of lift coefficient with horizontal-tail deflection, $\frac{\partial C_L}{\partial \delta_h}$, per radian

C_l rolling-moment coefficient, $\frac{\text{Rolling moment}}{\bar{q}Sb}$

C_{l_p} damping-in-roll derivative, $\frac{\partial C_l}{\partial \frac{pb}{2V}}$, per radian

C_{l_r} rate of change of rolling-moment coefficient with yawing angular-velocity factor, $\frac{\partial C_l}{\partial \frac{rb}{2V}}$, per radian

C_{l_β} effective dihedral derivative, $\frac{\partial C_l}{\partial \beta}$, per radian

$C_{l_{\dot{\beta}}}$ rate of change of rolling-moment coefficient with rate of change of angle-of-sideslip factor, $\frac{\partial C_l}{\partial \frac{\dot{\beta}b}{2V}}$, per radian

$C_{l_{\delta_a}}$ rate of change of rolling-moment coefficient with respect to aileron deflection, $\frac{\partial C_l}{\partial \delta_a}$, per radian

$C_{l_{\delta_v}}$ rate of change of rolling-moment coefficient with respect to vertical-tail deflection, $\frac{\partial C_l}{\partial \delta_v}$, per radian

C_m pitching-moment coefficient, $\frac{\text{Pitching moment}}{\bar{q}S\bar{c}}$

C_{m_0} pitching-moment coefficient at zero angle of attack

C_{m_α} longitudinal-stability derivative, $\frac{\partial C_m}{\partial \alpha}$, per radian

$C_{m_{\dot{\alpha}}}$ rate of change of pitching-moment coefficient with rate of change of angle-of-attack factor, $\frac{\partial C_m}{\partial \frac{\dot{\alpha}\bar{c}}{2V}}$, per radian

C_{m_β} rate of change of pitching-moment coefficient with angle of sideslip, $\frac{\partial C_m}{\partial \beta}$, per radian

C_{m_q} rate of change of pitching-moment coefficient with pitching angular-velocity factor, $\frac{\partial C_m}{\partial \frac{q\bar{c}}{2V}}$, per radian

$C_{m_{\delta_h}}$ rate of change of pitching-moment coefficient with respect to horizontal-tail deflection, $\frac{\partial C_m}{\partial \delta_h}$, per radian

C_n yawing-moment coefficient, $\frac{\text{Yawing moment}}{\bar{q}Sb}$

C_{n_p} rate of change of yawing-moment coefficient with rolling angular-velocity factor, $\frac{\partial C_n}{\partial \frac{pb}{2V}}$, per radian

C_{n_r} damping-in-yaw derivative, $\frac{\partial C_n}{\partial \frac{rb}{2V}}$, per radian

C_{n_β} directional-stability derivative, $\frac{\partial C_n}{\partial \beta}$, per radian

$C_{n_{\dot{\beta}}}$ rate of change of yawing-moment coefficient with rate of change of angle-of-sideslip factor, $\frac{\partial C_n}{\partial \frac{\dot{\beta} b}{2V}}$, per radian

$C_{n_{\delta_a}}$ rate of change of yawing-moment coefficient with respect to aileron deflection, $\frac{\partial C_n}{\partial \delta_a}$, per radian

$C_{n_{\delta_v}}$ rate of change of yawing-moment coefficient with respect to vertical-tail deflection, $\frac{\partial C_n}{\partial \delta_v}$, per radian

C_Y side-force coefficient, $\frac{\text{Side force}}{\bar{q}S}$

C_{Y_p} rate of change of side-force coefficient with rolling angular-velocity factor, $\frac{\partial C_Y}{\partial \frac{pb}{2V}}$, per radian

C_{Y_r} rate of change of side-force coefficient with yawing angular-velocity factor, $\frac{\partial C_Y}{\partial \frac{rb}{2V}}$, per radian

C_{Y_β} side-force derivative, $\frac{\partial C_Y}{\partial \beta}$, per radian

$C_{Y_{\dot{\beta}}}$ rate of change of side-force coefficient with rate of change of angle-of-sideslip factor, $\frac{\partial C_Y}{\partial \frac{\dot{\beta} b}{2V}}$, per radian

$C_{Y_{\delta_a}}$ rate of change of side-force coefficient with respect to aileron deflection, $\frac{\partial C_Y}{\partial \delta_a}$, per radian

$C_{Y_{\delta_v}}$ rate of change of side-force coefficient with respect to vertical-tail deflection, $\frac{\partial C_Y}{\partial \delta_v}$, per radian

$\bar{c}$	mean aerodynamic chord, ft
d	distance between center of gravity and main gear point of attachment measured in y-z plane parallel to z-axis, ft
d_1, d_2, d_N	distance between center of gravity and left main skid, right main skid, and nose skid, respectively, measured in y-z plane parallel to z-axis, ft
F_h	friction force on the landing gear, measured in the ground plane, lb
$F_{h_1}, F_{h_2}, F_{h_N}$	friction forces on the left main skid, right main skid, and nose skid, respectively, measured in the ground plane, lb
F_v	landing-gear reaction normal to the ground plane, lb
$F_{v_1}, F_{v_2}, F_{v_N}$	reactions of the left main gear, right main gear, and nose gear, respectively, normal to the ground plane, lb
F_x, F_y, F_z	force measured parallel to x-, y-, and z-axes, respectively, lb
h_1, h_2	distance between point of attachment and left main skid and right main skid, respectively, measured in the y-z plane parallel to the z_o-axis, ft
h_1', h_2'	distance between point of attachment and left main skid and right main skid, respectively, measured in the y_o-z_o plane parallel to the z_o-axis, ft
I_x, I_y, I_z	moments of inertia referred to the x-, y-, and z-axes, respectively, slug-ft^2
I_{xz}	product of inertia referred to the x- and z-axes, slug-ft^2
L_{HM}	distance between center of gravity and main gear point of attachment measured in x-z plane parallel to the x-axis, ft
l_{HN}	distance between center of gravity and nose gear point of attachment measured in x-z plane parallel to the x-axis, ft
l_1, l_2, l_N	distance between center of gravity and left main skid, right main skid, and nose skid, respectively, measured in x-z plane parallel to the x-axis, ft
M_x, M_y, M_z	moments about the x-, y-, and z-axes, respectively, ft-lb
m	vehicle mass, slugs
p, q, r	rolling, pitching, and yawing angular velocities, respectively, measured about the x-, y-, and z-axes, radian/sec

$\bar{q}$	dynamic pressure, $\frac{1}{2}\rho V^2$, lb/sq ft
S	wing area, sq ft
S_1, S_2	distance between center of gravity and left main gear and right main gear point of attachment, respectively, measured in the x-z plane parallel to the y-axis, ft
S_{A_1}, S_{A_2}	distance between center of gravity and left main skid and right main skid, respectively, measured in the x-z plane parallel to the y-axis, ft
t	time, sec
u,v,w	translational components of relative velocity vector parallel to x-, y-, and z-axes, respectively, ft/sec
u_w, v_w, w_w	components of wind velocity parallel to x-, y-, and z-axes, respectively, ft/sec
u_{w_o}, v_{w_o}	components of wind velocity relative to X- and Y-axes, respectively, ft/sec
u', v', w'	components of center-of-gravity translational velocity parallel to the x-, y-, and z-axes, respectively, ft/sec
V	magnitude of vehicle relative velocity, ft/sec
$\bar{V}$	vehicle relative-velocity vector, ft/sec
$\bar{V}'$	velocity vector of vehicle center of gravity relative to the ground, ft/sec
V_G	magnitude of relative-velocity vector measured in the ground plane, ft/sec
V_w	magnitude of wind velocity, ft/sec
$\bar{V}_w$	velocity vector of wind relative to the ground, ft/sec
V'_x, V'_y, V'_z	components of center-of-gravity velocity, relative to x-, y-, and z-axes, respectively, ft/sec
V'_{x_o}, V'_{y_o}	components of center-of-gravity velocity parallel to the x_o- and y_o-axes, respectively, ft/sec
W	vehicle weight, lb
X,Y,Z	fixed-earth cartesian coordinate system
x,y,z	cartesian coordinates of body axis system

x_o, y_o, z_o	cartesian coordinates obtained by rotating X-, Y-, and Z-system through Euler angle ψ; distances measured parallel to these axes, ft
α	angle of attack, radians
β	angle of sideslip, radians
β'	angle measured between V_G and x_o-axis, radians
γ	angle defined by equation (11), radians
δ_a	aileron deflection, radians
δ_h	horizontal-tail (elevator) deflection, radians
δ_v	vertical-tail (rudder) deflection, radians
$\delta_{M_1}, \delta_{M_2}$	change in vertical height of left and right main gear, respectively, ft
ϵ	length of time increment, sec
$\lambda_1, \lambda_2, \lambda_N$	angle between the x_o-axis and the friction force on the left main skid, right main skid, and nose skid, respectively, radians
μ	coefficient of friction for a skid
μ_1, μ_N	coefficient of friction for the main skids and nose skid, respectively
ρ	density of air, slugs/cu ft
ψ, θ, φ	Euler yaw, pitch, and roll angle, respectively, radians
ψ_w	angle between wind velocity vector and X-axis, radians

Subscripts:

i	refers to body position or skid being considered
n,n-1,n+1	time interval being considered in numerical integration, n=0, 1, 2, 3...
aero	aerodynamic inputs only
gear	landing gear only
touchdown	quantity measured at touchdown

A dot above a quantity denotes the first derivative with respect to time. A double dot above a quantity denotes the second derivative with respect to time.

ANALYSIS

Slideout Equations for a Vehicle With Three Skid-Type Landing Gear

The equations of motion are presented for the slideout of a vehicle with a tricycle landing-gear system equipped with skids. The vehicle geometry, body-axis coordinate system, and directions of friction forces and gear reactions used in this analysis are shown in figure 1. The x-, y-, and z-body axes, originating

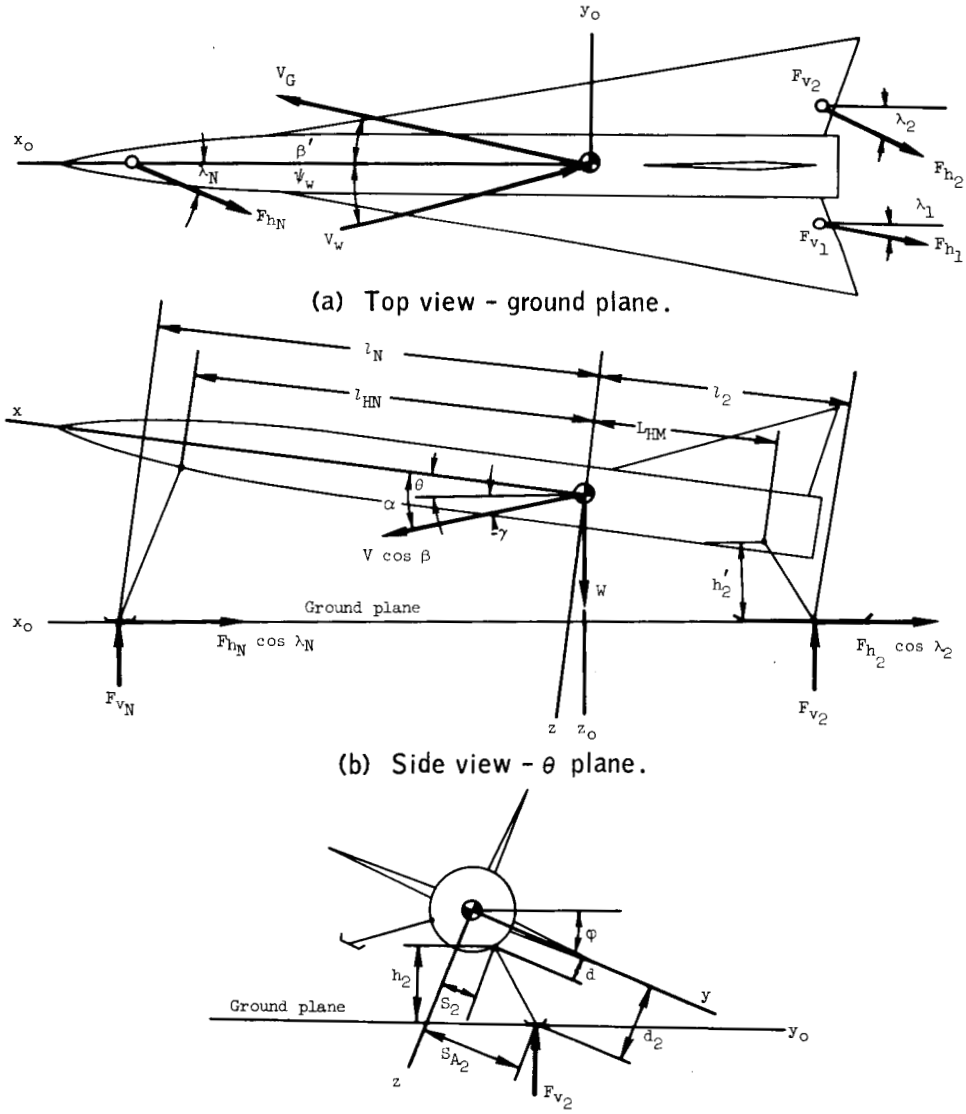

Figure 1.- Vehicle geometry and gear loadings.

at the center of gravity, are chosen so that the x-z plane is the vehicle plane of symmetry. The friction force F_h lies in the ground plane and the gear reaction F_v is normal to this plane.

The transformation from a fixed-earth system of coordinate axes X, Y, and Z to the body axes x, y, and z is illustrated in figure 2. A rotation about the Z-axis through the Euler yaw angle ψ results in the coordinate system x_o, y_o, z_o. The x, y, z system is obtained by rotating the x_o, y_o, z_o system, first through the Euler pitch angle θ, and then through the roll angle φ. Thus, the ground-plane components of the x-, y-, z-axes lie in the x_o, y_o, z_o system. The transformation is dependent upon the order of rotation which, for this analysis, is ψ, θ, and φ.

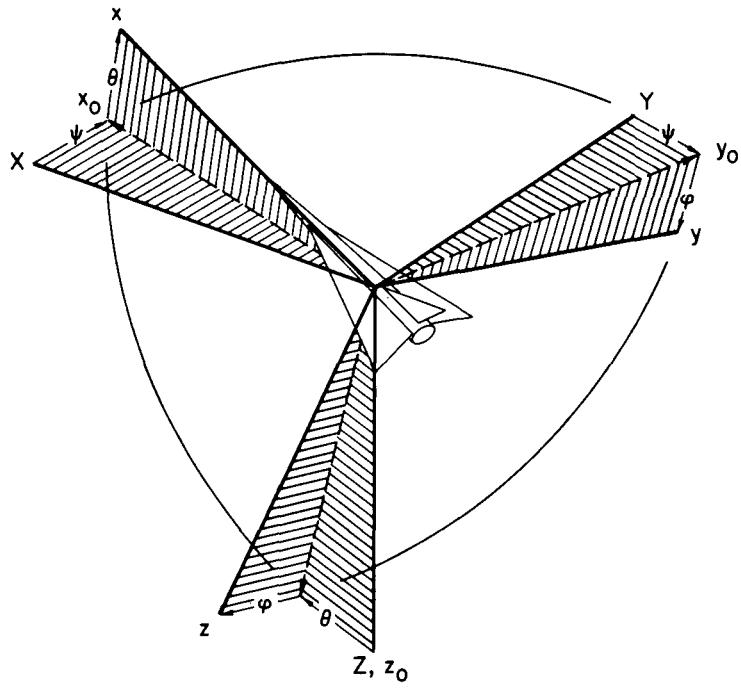

Figure 2.- Orientation of body axes with respect to earth axes.

Referring to figures 1 and 2, and resolving friction forces and gear reactions into components parallel to the body axes, the following equations, referred to the body axes, are obtained for the contribution of the landing-gear forces to the total forces and moments on the vehicle:

$$\Sigma F_{x_{gear}} = -\left(F_{h_1}\cos\lambda_1 + F_{h_2}\cos\lambda_2 + F_{h_N}\cos\lambda_N\right)\cos\theta + \left(F_{v_1} + F_{v_2} + F_{v_N}\right)\sin\theta \tag{1a}$$

$$\Sigma F_{y_{gear}} = -F_{h_1}\left(\cos\varphi\sin\lambda_1 + \sin\theta\sin\varphi\cos\lambda_1\right) - F_{h_2}\left(\cos\varphi\sin\lambda_2 + \sin\theta\sin\varphi\cos\lambda_2\right)$$
$$- F_{h_N}\left(\cos\varphi\sin\lambda_N + \sin\theta\sin\varphi\cos\lambda_N\right) - \left(F_{v_1} + F_{v_2} + F_{v_N}\right)\cos\theta\sin\varphi \tag{1b}$$

$$\Sigma F_{z_{gear}} = -F_{h_1}\left(\sin\theta\cos\varphi\cos\lambda_1 - \sin\varphi\sin\lambda_1\right) - F_{h_2}\left(\sin\theta\cos\varphi\cos\lambda_2 - \sin\varphi\sin\lambda_2\right)$$
$$- F_{h_N}\left(\sin\theta\cos\varphi\cos\lambda_N - \sin\varphi\sin\lambda_N\right) - \left(F_{v_1} + F_{v_2} + F_{v_N}\right)\cos\theta\cos\varphi \tag{1c}$$

$$\Sigma M_{x_{gear}} = F_{h_1}\Big[\big(S_{A_1}\cos\varphi + d_1\sin\varphi\big)\sin\theta\cos\lambda_1 - \big(S_{A_1}\sin\varphi - d_1\cos\varphi\big)\sin\lambda_1\Big]$$
$$- F_{h_2}\Big[\big(S_{A_2}\cos\varphi - d_2\sin\varphi\big)\sin\theta\cos\lambda_2 - \big(S_{A_2}\sin\varphi + d_2\cos\varphi\big)\sin\lambda_2\Big]$$
$$+ F_{h_N}d_N\big(\cos\varphi\sin\lambda_N + \sin\theta\sin\varphi\cos\lambda_N\big) + F_{v_1}\big(S_{A_1}\cos\varphi + d_1\sin\varphi\big)\cos\theta$$
$$- F_{v_2}\big(S_{A_2}\cos\varphi - d_2\sin\varphi\big)\cos\theta + F_{v_N}d_N\cos\theta\sin\varphi \qquad (1d)$$

$$\Sigma M_{y_{gear}} = F_{h_1}\Big[l_1\sin\varphi\sin\lambda_1 - \big(l_1\sin\theta\cos\varphi + d_1\cos\theta\big)\cos\lambda_1\Big]$$
$$+ F_{h_2}\Big[l_2\sin\varphi\sin\lambda_2 - \big(l_2\sin\theta\cos\varphi + d_2\cos\theta\big)\cos\lambda_2\Big]$$
$$- F_{h_N}\Big[l_N\sin\varphi\sin\lambda_N - \big(l_N\sin\theta\cos\varphi - d_N\cos\theta\big)\cos\lambda_N\Big]$$
$$+ F_{v_1}\big(d_1\sin\theta - l_1\cos\theta\cos\varphi\big) + F_{v_2}\big(d_2\sin\theta - l_2\cos\theta\cos\varphi\big)$$
$$+ F_{v_N}\big(d_N\sin\theta + l_N\cos\theta\cos\varphi\big) \qquad (1e)$$

$$\Sigma M_{z_{gear}} = F_{h_1}\Big[l_1\cos\varphi\sin\lambda_1 + \big(l_1\sin\theta\sin\varphi - S_{A_1}\cos\theta\big)\cos\lambda_1\Big]$$
$$+ F_{h_2}\Big[l_2\cos\varphi\sin\lambda_2 + \big(l_2\sin\theta\sin\varphi + S_{A_2}\cos\theta\big)\cos\lambda_2\Big]$$
$$- F_{h_N}l_N\big(\cos\varphi\sin\lambda_N + \sin\theta\sin\varphi\cos\lambda_N\big)$$
$$+ F_{v_1}\big(S_{A_1}\sin\theta + l_1\cos\theta\sin\varphi\big) - F_{v_2}\big(S_{A_2}\sin\theta - l_2\cos\theta\sin\varphi\big)$$
$$- F_{v_N}l_N\cos\theta\sin\varphi \qquad (1f)$$

Aerodynamic forces and moments, referred to body axes, are of the form normally used in airplane stability analysis (ref. 10) and are written as:

$$\Sigma F_{x_{aero}} = \bar{q}S\big(C_L\sin\theta - C_D\cos\theta\big) \qquad (2a)$$

$$\Sigma F_{y_{aero}} = \bar{q}S\Big[C_{Y_{\delta_a}}\delta_a + C_{Y_{\delta_v}}\delta_v + C_{Y_\beta}\beta + \frac{b}{2V}\big(C_{Y_r}r + C_{Y_p}p + C_{Y_{\dot\beta}}\dot\beta\big)\Big] \qquad (2b)$$

$$\Sigma F_{z_{aero}} = -\bar{q}S\left(C_L \cos\theta + C_D \sin\theta\right) \tag{2c}$$

$$\Sigma M_{x_{aero}} = \bar{q}Sb\left[C_{l_{\delta_a}}\delta_a + C_{l_{\delta_v}}\delta_v + C_{l_\beta}\beta + \frac{b}{2V}\left(C_{l_p}p + C_{l_r}r + C_{l_{\dot\beta}}\dot\beta\right)\right] \tag{2d}$$

$$\Sigma M_{y_{aero}} = \bar{q}S\bar{c}\left[C_{m_{\delta_h}}\delta_h + C_{m_0} + C_{m_\alpha}\alpha + C_{m_\beta}\beta + \frac{\bar{c}}{2V}\left(C_{m_q}q + C_{m_{\dot\alpha}}\dot\alpha\right)\right] \tag{2e}$$

$$\Sigma M_{z_{aero}} = \bar{q}Sb\left[C_{n_{\delta_a}}\delta_a + C_{n_{\delta_v}}\delta_v + C_{n_\beta}\beta + \frac{b}{2V}\left(C_{n_p}p + C_{n_r}r + C_{n_{\dot\beta}}\dot\beta\right)\right] \tag{2f}$$

The total forces and moments on the vehicle during slideout are obtained by adding inertia and weight contributions to the sums of equations (1) and (2). Thus, the equilibrium equations referred to the vehicle body axes are:

$$\Sigma F_x = -m(\dot u + qw - rv) + \bar{q}S\left(C_L \sin\theta - C_D \cos\theta\right) + \left(F_{v_1} + F_{v_2} + F_{v_N}\right)\sin\theta$$
$$-\left(F_{h_1}\cos\lambda_1 + F_{h_2}\cos\lambda_2 + F_{h_N}\cos\lambda_N\right)\cos\theta - W\sin\theta = 0 \tag{3a}$$

$$\Sigma F_y = -m(\dot v + ru - pw) + \bar{q}S\left[C_{Y_{\delta_a}}\delta_a + C_{Y_{\delta_v}}\delta_v + C_{Y_\beta}\beta + \frac{b}{2V}\left(C_{Y_r}r + C_{Y_p}p + C_{Y_{\dot\beta}}\dot\beta\right)\right]$$
$$-\left(F_{v_1} + F_{v_2} + F_{v_N}\right)\cos\theta\sin\varphi - F_{h_1}\left(\cos\varphi\sin\lambda_1 + \sin\theta\sin\varphi\cos\lambda_1\right)$$
$$-F_{h_2}\left(\cos\varphi\sin\lambda_2 + \sin\theta\sin\varphi\cos\lambda_2\right) - F_{h_N}\left(\cos\varphi\sin\lambda_N + \sin\theta\sin\varphi\cos\lambda_N\right)$$
$$+W\cos\theta\sin\varphi = 0 \tag{3b}$$

$$\Sigma F_z = -m(\dot w + pv - qu) - \bar{q}S\left(C_L\cos\theta + C_D\sin\theta\right) - \left(F_{v_1} + F_{v_2} + F_{v_N}\right)\cos\theta\cos\varphi$$
$$-F_{h_1}\left(\sin\theta\cos\varphi\cos\lambda_1 - \sin\varphi\sin\lambda_1\right) - F_{h_2}\left(\sin\theta\cos\varphi\cos\lambda_2 - \sin\varphi\sin\lambda_2\right)$$
$$-F_{h_N}\left(\sin\theta\cos\varphi\cos\lambda_N - \sin\varphi\sin\lambda_N\right) + W\cos\theta\cos\varphi = 0 \tag{3c}$$

$$\Sigma M_x = -I_x\dot{p} + I_{xz}(\dot{r} + pq) + \left(I_y - I_z\right)qr + \bar{q}Sb\Big[C_{l_{\delta_a}}\delta_a + C_{l_{\delta_v}}\delta_v + C_{l_\beta}\beta$$

$$+ \frac{b}{2V}\left(C_{l_p}p + C_{l_r}r + C_{l_{\dot{\beta}}}\dot{\beta}\right)\Big] + F_{v_1}\left(S_{A_1}\cos\varphi + d_1\sin\varphi\right)\cos\theta$$

$$- F_{v_2}\left(S_{A_2}\cos\varphi - d_2\sin\varphi\right)\cos\theta + F_{v_N}d_N\cos\theta\sin\varphi$$

$$+ F_{h_1}\Big[\left(S_{A_1}\cos\varphi + d_1\sin\varphi\right)\sin\theta\cos\lambda_1 - \left(S_{A_1}\sin\varphi - d_1\cos\varphi\right)\sin\lambda_1\Big]$$

$$- F_{h_2}\Big[\left(S_{A_2}\cos\varphi - d_2\sin\varphi\right)\sin\theta\cos\lambda_2 - \left(S_{A_2}\sin\varphi + d_2\cos\varphi\right)\sin\lambda_2\Big]$$

$$+ F_{h_N}d_N\left(\cos\varphi\sin\lambda_N + \sin\theta\sin\varphi\cos\lambda_N\right) = 0 \qquad (3d)$$

$$\Sigma M_y = -I_y\dot{q} + \left(I_z - I_x\right)pr + I_{xz}\left(r^2 - p^2\right) + \bar{q}S\bar{c}\Big[C_{m_{\delta_h}}\delta_h + C_{m_0} + C_{m_\alpha}\alpha$$

$$+ C_{m_\beta}\beta + \frac{\bar{c}}{2V}\left(C_{m_q}q + C_{m_{\dot{\alpha}}}\dot{\alpha}\right)\Big] + F_{v_1}\left(d_1\sin\theta - l_1\cos\theta\cos\varphi\right)$$

$$+ F_{v_2}\left(d_2\sin\theta - l_2\cos\theta\cos\varphi\right) + F_{v_N}\left(d_N\sin\theta + l_N\cos\theta\cos\varphi\right)$$

$$+ F_{h_1}\Big[l_1\sin\varphi\sin\lambda_1 - \left(l_1\sin\theta\cos\varphi + d_1\cos\theta\right)\cos\lambda_1\Big]$$

$$+ F_{h_2}\Big[l_2\sin\varphi\sin\lambda_2 - \left(l_2\sin\theta\cos\varphi + d_2\cos\theta\right)\cos\lambda_2\Big]$$

$$- F_{h_N}\Big[l_N\sin\varphi\sin\lambda_N - \left(l_N\sin\theta\cos\varphi - d_N\cos\theta\right)\cos\lambda_N\Big] = 0 \qquad (3e)$$

$$\Sigma M_z = -I_z\dot{r} + I_{xz}(\dot{p} - qr) + \left(I_x - I_y\right)pq + \bar{q}Sb\Big[C_{n_{\delta_a}}\delta_a + C_{n_{\delta_v}}\delta_v + C_{n_\beta}\beta$$

$$+ \frac{b}{2V}\left(C_{n_r}r + C_{n_p}p + C_{n_{\dot{\beta}}}\dot{\beta}\right)\Big] + F_{v_1}\left(S_{A_1}\sin\theta + l_1\cos\theta\sin\varphi\right)$$

$$- F_{v_2}\left(S_{A_2}\sin\theta - l_2\cos\theta\sin\varphi\right) - F_{v_N}l_N\cos\theta\sin\varphi$$

$$+ F_{h_1}\Big[l_1\cos\varphi\sin\lambda_1 + \left(l_1\sin\theta\sin\varphi - S_{A_1}\cos\theta\right)\cos\lambda_1\Big]$$

$$+ F_{h_2}\Big[l_2\cos\varphi\sin\lambda_2 + \left(l_2\sin\theta\sin\varphi + S_{A_2}\cos\theta\right)\cos\lambda_2\Big]$$

$$- F_{h_N}l_N\left(\cos\varphi\sin\lambda_N + \sin\theta\sin\varphi\cos\lambda_N\right) = 0 \qquad (3f)$$

The skid friction force is proportional to the gear reaction normal to the ground and is expressed as:

$$F_h = \mu F_v \tag{4}$$

For most applications the coefficient of friction μ is considered to be constant; however, it may vary with velocity and temperature as shown in references 7 and 11. Since the main skids on a reentry vehicle are expected to be constructed of the same material, the coefficients of friction for these skids are considered to be identical. The nose-gear skid may be made of a material with a coefficient of friction different from that for the main skids. Thus, the friction forces, in the form of equation (4), may be written as:

$$\left.\begin{aligned} F_{h_1} &= \mu_1 F_{v_1} \\ F_{h_2} &= \mu_1 F_{v_2} \\ F_{h_N} &= \mu_N F_{v_N} \end{aligned}\right\} \tag{5}$$

The dynamics of transformations between earth-fixed and body coordinates yield the following equations relating body and Euler rotational rates (see ref. 12):

$$\left.\begin{aligned} p &= \dot{\varphi} - \dot{\psi} \sin \theta \\ q &= \dot{\theta} \cos \varphi + \dot{\psi} \cos \theta \sin \varphi \\ r &= \dot{\psi} \cos \theta \cos \varphi - \dot{\theta} \sin \varphi \end{aligned}\right\} \tag{6}$$

The relative velocity and the components of relative velocity are related through the sideslip angle and the angle of attack. By definition,

$$\left.\begin{aligned} \beta &= \sin^{-1} \frac{v}{V} \\ \alpha &= \tan^{-1} \frac{w}{u} \end{aligned}\right\} \tag{7}$$

and

As a result of equations (7), the relative-velocity components and their time derivatives are:

$$\left.\begin{aligned} v &= V \sin \beta \\ u &= V \cos \beta \cos \alpha \\ w &= V \cos \beta \sin \alpha \\ \dot{v} &= \dot{V} \sin \beta + V\dot{\beta} \cos \beta \\ \dot{u} &= \dot{V} \cos \beta \cos \alpha - V(\dot{\beta} \sin \beta \cos \alpha + \dot{\alpha} \cos \beta \sin \alpha) \\ \dot{w} &= \dot{V} \cos \beta \sin \alpha - V(\dot{\beta} \sin \beta \sin \alpha - \dot{\alpha} \cos \beta \cos \alpha) \end{aligned}\right\} \quad (8)$$

In general, the landing gear will deflect and bend as the loads on the gear vary during landing and slideout. The rate of change of total vertical gear deflection can be related to the vertical velocity of the center of gravity as shown in appendix A. The results of appendix A are used to determine the gear deflection which is related to the gear loading. One method of determining the relationship between the total vertical deflection and gear loading is to conduct tests of the actual hardware. Thus, the gear loading which causes a specific deflection can be found. In addition, the moment arms from the center of gravity to the skids can be corrected as the gear deflect and bend.

The vertical velocity $\dot{z}_o$ of the center of gravity is related to the vehicle geometry and rate of vertical deflection of the gear by equations (A3) and (A4) and to the relative-velocity components by (see ref. 13):

$$\dot{z}_o = -u \sin \theta + v \sin \varphi \cos \theta + w \cos \varphi \cos \theta \quad (9)$$

The angle of attack is related to the vertical velocity of the center of gravity by

$$\alpha = \theta - \gamma \quad (10)$$

where γ, referring to the vehicle attitude, is expressed as

$$\gamma = \sin^{-1} \frac{\dot{z}_o}{V \cos \beta} \quad (11)$$

Additional equations are required if the elasticity of the vehicle structure, as well as that of the landing gear, is to be taken into account. These elastic conditions are not considered in this paper.

Simplified Slideout Equations for a Vehicle With Three Skid-Type Landing Gear

A practical approximation to the equations of motion presented in the preceding section may be obtained from the assumptions that the vehicle has rigid gear during slideout and that all skids must remain in contact with the ground at all times. These assumptions are valid if (1) the vehicle is sliding on a flat surface, (2) the initial landing-impact oscillations have been damped, and (3) gear deflections resulting from all other inputs are negligible.

The above assumptions imply that the roll and pitch rates must be zero; therefore, the roll and pitch attitudes remain constant. In addition, since it has been assumed that the vehicle is symmetrical about the x-z plane and that the geometry of the main gear is identical, the roll angle must be zero. These physical restraints on the vehicle attitude during slideout are stated as

$$\left.\begin{aligned} &\dot{\theta} = 0, \qquad \dot{\varphi} = 0 \\ &\text{and} \\ &\theta = \text{constant}, \qquad \varphi = \text{constant} = 0 \end{aligned}\right\} \tag{12}$$

The symmetry of the vehicle and the assumption of rigid gear also imply that

$$\left.\begin{aligned} &d_1 = d_2 \\ &\text{and} \\ &l_1 = l_2 \end{aligned}\right\} \tag{13}$$

Since the center of gravity cannot have any vertical motion as a result of the previously stated assumptions, and if it is assumed that any existing wind blows parallel to the ground plane, the velocity of the vehicle relative to the airstream during slideout will be parallel to the ground plane. Consequently, equation (10) becomes

$$\left.\begin{aligned} &\alpha = \theta = \text{constant} \\ &\text{and} \\ &\dot{\alpha} = 0 \end{aligned}\right\} \tag{14}$$

The substitution of equations (5), (6), and (8) into the equilibrium equations (3) yields, upon the application of equations (12) to (14), the following equations for the slideout of a vehicle with a tricycle, rigid, skid-type landing-gear system:

$$\Sigma F_x = m\left[\dot{V}\cos\beta - (\dot{\beta}+\dot{\psi})V\sin\beta\right]\cos\theta + \tfrac{1}{2}\rho V^2 S\left(C_D\cos\theta - C_L\sin\theta\right)$$
$$+ \left(\mu_1\cos\theta\cos\lambda_1 - \sin\theta\right)F_{v_1} + \left(\mu_1\cos\theta\cos\lambda_2 - \sin\theta\right)F_{v_2}$$
$$+ \left(\mu_N\cos\theta\cos\lambda_N - \sin\theta\right)F_{v_N} + W\sin\theta = 0 \qquad (15a)$$

$$\Sigma F_y = m\left[\dot{V}\sin\beta + (\dot{\beta}+\dot{\psi})V\cos\beta\right] - \tfrac{1}{2}\rho V^2 S\left[C_{Y_{\delta_a}}\delta_a + C_{Y_{\delta_v}}\delta_v + C_{Y_\beta}\beta\right.$$
$$\left. + \frac{b}{2V}\left(C_{Y_r}\dot{\psi}\cos\theta - C_{Y_p}\dot{\psi}\sin\theta + C_{Y_{\dot{\beta}}}\dot{\beta}\right)\right] + \mu_1\sin\lambda_1 F_{v_1}$$
$$+ \mu_1\sin\lambda_2 F_{v_2} + \mu_N\sin\lambda_N F_{v_N} = 0 \qquad (15b)$$

$$\Sigma F_z = m\left[\dot{V}\cos\beta - (\dot{\beta}+\dot{\psi})V\sin\beta\right]\sin\theta + \tfrac{1}{2}\rho V^2 S\left(C_L\cos\theta + C_D\sin\theta\right)$$
$$+ \left(\mu_1\sin\theta\cos\lambda_1 + \cos\theta\right)F_{v_1} + \left(\mu_1\sin\theta\cos\lambda_2 + \cos\theta\right)F_{v_2}$$
$$+ \left(\mu_N\sin\theta\cos\lambda_N + \cos\theta\right)F_{v_N} - W\cos\theta = 0 \qquad (15c)$$

$$\Sigma M_x = \left(I_x\sin\theta + I_{xz}\cos\theta\right)\ddot{\psi} + \tfrac{1}{2}\rho V^2 Sb\left[C_{l_{\delta_a}}\delta_a + C_{l_{\delta_v}}\delta_v + C_{l_\beta}\beta\right.$$
$$\left. + \frac{b}{2V}\left(C_{l_r}\dot{\psi}\cos\theta - C_{l_p}\dot{\psi}\sin\theta + C_{l_{\dot{\beta}}}\dot{\beta}\right)\right]$$
$$+ \left[\mu_1\left(S_{A_1}\sin\theta\cos\lambda_1 + d_1\sin\lambda_1\right) + S_{A_1}\cos\theta\right]F_{v_1}$$
$$- \left[\mu_1\left(S_{A_2}\sin\theta\cos\lambda_2 - d_1\sin\lambda_2\right) + S_{A_2}\cos\theta\right]F_{v_2}$$
$$+ \mu_N d_N\sin\lambda_N F_{v_N} = 0 \qquad (15d)$$

$$\Sigma M_y = \left[\left(I_x - I_z\right)\sin\theta\cos\theta + I_{xz}\left(\cos^2\theta - \sin^2\theta\right)\right]\dot{\psi}^2$$

$$+ \frac{1}{2}\rho V^2 S\bar{c}\left(C_{m_{\delta_h}}\delta_h + C_{m_0} + C_{m_\alpha}\theta + C_{m_\beta}\beta\right)$$

$$+ \left[d_1\left(\sin\theta - \mu_1\cos\theta\cos\lambda_1\right) - l_1\left(\cos\theta + \mu_1\sin\theta\cos\lambda_1\right)\right]F_{v_1}$$

$$+ \left[d_1\left(\sin\theta - \mu_1\cos\theta\cos\lambda_2\right) - l_1\left(\cos\theta + \mu_1\sin\theta\cos\lambda_2\right)\right]F_{v_2}$$

$$+ \left[d_N\left(\sin\theta - \mu_N\cos\theta\cos\lambda_N\right) + l_N\left(\cos\theta + \mu_N\sin\theta\cos\lambda_N\right)\right]F_{v_N} = 0 \quad (15e)$$

$$\Sigma M_z = -\left(I_z\cos\theta + I_{xz}\sin\theta\right)\ddot{\psi} + \frac{1}{2}\rho V^2 Sb\left[C_{n_{\delta_a}}\delta_a + C_{n_{\delta_v}}\delta_v + C_{n_\beta}\beta\right.$$

$$\left. + \frac{b}{2V}\left(C_{n_r}\dot{\psi}\cos\theta - C_{n_p}\dot{\psi}\sin\theta + C_{n_{\dot{\beta}}}\dot{\beta}\right)\right]$$

$$+ \left[\mu_1\left(l_1\sin\lambda_1 - S_{A_1}\cos\theta\cos\lambda_1\right) + S_{A_1}\sin\theta\right]F_{v_1}$$

$$+ \left[\mu_1\left(l_1\sin\lambda_2 + S_{A_2}\cos\theta\cos\lambda_2\right) - S_{A_2}\sin\theta\right]F_{v_2}$$

$$- \mu_N l_N\sin\lambda_N F_{v_N} = 0 \quad (15f)$$

The trigonometric relations for λ_1, λ_2, and λ_N are derived in appendix B. These relations, given by equations (B1), (B8), and (B9), yield the angles as functions of relative velocity, sideslip angle, and body yaw rate. Thus, the six simplified slideout equations (15) are in terms of six variables: V, β, ψ, F_{v_1}, F_{v_2}, and F_{v_N}.

Simplified Slideout Equations for a Vehicle in a Low Pitch Attitude

The equations of motions for slideout can be further simplified if the vehicle is in a low pitch attitude, that is, low angle of attack. Since the pitch angle is small, the following simplifications can be used:

1. The trigonometric relations may be written as

$$\sin\theta \approx \theta$$

$$\cos\theta \approx 1$$

2. The z-component of relative velocity is small compared to the x- and y-components. Therefore,

$$w \approx 0$$

$$\dot{w} \approx 0$$

3. Retaining only significant terms, equations (6) and their derivatives become for the slideout condition

$$p \approx 0 \qquad \dot{p} \approx 0$$

$$q = 0 \qquad \dot{q} = 0$$

$$r \approx \dot{\psi} \qquad \dot{r} \approx \ddot{\psi}$$

If the above simplifications are applied to the basic slideout equations (15), they become:

$$\Sigma F_x = \left(m \cos \beta\right)\dot{V} - \left(mV \sin \beta\right)\dot{\beta} - mrV \sin \beta + \frac{\rho S}{2}\left(C_D - C_L\theta\right)V^2$$
$$+ \left(\mu_1 \cos \lambda_1 - \theta\right)F_{v_1} + \left(\mu_1 \cos \lambda_2 - \theta\right)F_{v_2} + \left(\mu_N \cos \lambda_N - \theta\right)F_{v_N}$$
$$+ W\theta = 0 \tag{16a}$$

$$\Sigma F_y = \left(m \sin \beta\right)\dot{V} + \left(mV \cos \beta\right)\dot{\beta} + mrV \cos \beta - \frac{\rho S}{2}\left[C_{Y_{\delta_a}}\delta_a + C_{Y_{\delta_v}}\delta_v + C_{Y_\beta}\beta\right.$$
$$\left. + \frac{b}{2V}\left(C_{Y_r}r + C_{Y_{\dot{\beta}}}\dot{\beta}\right)\right]V^2 + \left(\mu_1 \sin \lambda_1\right)F_{v_1} + \left(\mu_1 \sin \lambda_2\right)F_{v_2}$$
$$+ \left(\mu_N \sin \lambda_N\right)F_{v_N} = 0 \tag{16b}$$

$$\Sigma F_z = \frac{\rho S}{2}\left(C_L + C_D\theta\right)V^2 + \left(\mu_1\theta \cos \lambda_1 + 1\right)F_{v_1} + \left(\mu_1\theta \cos \lambda_2 + 1\right)F_{v_2}$$
$$+ \left(\mu_N\theta \cos \lambda_N + 1\right)F_{v_N} - W = 0 \tag{16c}$$

$$\Sigma M_x = I_{xz}\dot{r} + \frac{\rho Sb}{2}\left[C_{l_{\delta_a}}\delta_a + C_{l_{\delta_v}}\delta_v + C_{l_\beta}\beta + \frac{b}{2V}\left(C_{l_r}r + C_{l_{\dot{\beta}}}\dot{\beta}\right)\right]V^2$$
$$+ \left[\mu_1\left(S_{A_1}\theta\cos\lambda_1 + d_1\sin\lambda_1\right) + S_{A_1}\right]F_{v_1}$$
$$- \left[\mu_1\left(S_{A_2}\theta\cos\lambda_2 - d_1\sin\lambda_2\right) + S_{A_2}\right]F_{v_2} + \left(\mu_N d_N\sin\lambda_N\right)F_{v_N} = 0 \qquad (16d)$$

$$\Sigma M_y = I_{xz}r^2 + \frac{\rho S\bar{c}}{2}\left(C_{m_{\delta_h}}\delta_h + C_{m_0} + C_{m_\alpha}\theta + C_{m_\beta}\beta\right)V^2$$
$$+ \left[d_1\left(\theta - \mu_1\cos\lambda_1\right) - l_1\left(1 + \mu_1\theta\cos\lambda_1\right)\right]F_{v_1}$$
$$+ \left[d_1\left(\theta - \mu_1\cos\lambda_2\right) - l_1\left(1 + \mu_1\theta\cos\lambda_2\right)\right]F_{v_2}$$
$$+ \left[d_N\left(\theta - \mu_N\cos\lambda_N\right) + l_N\left(1 + \mu_N\theta\cos\lambda_N\right)\right]F_{v_N} = 0 \qquad (16e)$$

$$\Sigma M_z = -I_z\dot{r} + \frac{\rho Sb}{2}\left[C_{n_{\delta_a}}\delta_a + C_{n_{\delta_v}}\delta_v + C_{n_\beta}\beta + \frac{b}{2V}\left(C_{n_r}r + C_{n_{\dot{\beta}}}\dot{\beta}\right)\right]V^2$$
$$+ \left[\mu_1\left(l_1\sin\lambda_1 - S_{A_1}\cos\lambda_1\right) + S_{A_1}\theta\right]F_{v_1}$$
$$+ \left[\mu_1\left(l_1\sin\lambda_2 + S_{A_2}\cos\lambda_2\right) - S_{A_2}\theta\right]F_{v_2} - \left(\mu_N l_N\sin\lambda_N\right)F_{v_N} = 0 \qquad (16f)$$

Equations (16), upon application of the trigonometric relations from equations (B1), (B8), and (B10), can be solved, yielding equations for $\dot{V}$, $\dot{\beta}$, and $\dot{r}$. Because of the complexity of the resulting nonlinear differential equations, numerical methods are used to obtain a solution. The finite-difference technique described in reference 14 was used. Initial conditions and equations for determining the slideout distance are given in appendix C.

RESULTS AND DISCUSSION

The slideout dynamics of a space vehicle equipped with a tricycle skid-type landing-gear system are presented in the basic equations (3). These equations describe the general motion of the vehicle during slideout, including rolling, pitching, and yawing motions, variable aerodynamics, and variable coefficients of friction. Additional motion caused by structural flexibility of the landing gear is considered in appendix A. The basic equations are simplified to three degrees of freedom in equations (15) if the vehicle has rigid gear and if all skids remain in contact with the ground at all times during slideout. These

simplifying assumptions can be verified from model tests for vehicles of various configurations. The complexity of equations (15), as a result of nonlinearity and coupled motion, can be reduced if the vehicle is at a low angle of attack during slideout as presented in equations (16). The general motion equations (3) can be used to predict the slideout characteristics as well as the stability and controllability of the vehicle during slideout. Equations (15) and (16) have been derived by assuming that the vehicle is inherently stable, that is, it will not pitch or roll. These equations can be used to predict slideout characteristics and controllability.

In order to ascertain the validity of the theoretical investigation, results of calculations performed for equations (16) are compared to experimental slideout data obtained from the X-15 research vehicle. The X-15 is shown during slideout in figure 3. Numerical calculations were made on a digital computer, using the geometry and aerodynamic coefficients of the X-15 listed in the following table:

Geometry	
$b = 22.36$ ft	$l_N = 23.20$ ft
$\bar{c} = 10.30$ ft	$S = 200$ sq ft
$d_1 = 5.184$ ft	$S_{A_1} = 5.10$ ft
$d_2 = 5.184$ ft	$S_{A_2} = 5.10$ ft
$d_N = 3.583$ ft	$\mu_1 = 0.28$
$l_1 = 15.90$ ft	$\mu_N = 0.04$
$l_2 = 15.90$ ft	$\theta = -2.35°$
Aerodynamics	
$C_D = 0.120$ where $\delta_h = 0°$	$C_{m_{\delta_h}} = -1.320$ per radian
$C_{D_{\delta_h}} = 0.105$ per radian	$C_{n_r} - C_{n_{\dot{\beta}}} = -1.350$ per radian
$C_L = -0.050$ where $\delta_h = 0°$	$C_{n_\beta} = 0.280$ per radian
$C_{L_{\delta_h}} = 0.975$ per radian	$C_{n_{\delta_a}} = 0.077$ per radian
$C_{l_r} - C_{l_{\dot{\beta}}} = -0.020$ per radian	$C_{n_{\delta_v}} = -0.149$ per radian
$C_{l_\beta} = 0.023$ per radian	$C_{Y_r} - C_{Y_{\dot{\beta}}}$ Considered negligible
$C_{l_{\delta_a}} = 0.097$ per radian	$C_{Y_\beta} = -1.140$ per radian
$C_{l_{\delta_v}} = 0.032$ per radian	$C_{Y_{\delta_a}} = -0.100$ per radian
$C_{m_0} + C_{m_\alpha}\alpha = 0.050$ per radian	$C_{Y_{\delta_v}} = 0.240$ per radian
C_{m_β} Considered negligible	

Figure 3.- Attitude of X-15 airplane during slideout (photo taken from motion-picture sequence).

Positive directions for the aerodynamic coefficients are shown in figure 4. Equations (16) are made more amenable to calculation processes by assuming that during slideout all aerodynamic derivatives and the coefficients of friction are constant. In addition, the products of inertia of the X-15 airplane are negligible compared to the moments of inertia. The trigonometric relations given in appendix B are valid for the main gear; however, a fully castering nosewheel which alines itself to the direction of relative motion of the center of gravity is used on the X-15. Thus, for the nose gear, the angle λ_N is approximately equal to the sideslip angle β.

Numerical calculations were made by utilizing slideout data from the X-15 research vehicle. A flight was selected in which the pilot varied the control positions during the slideout to determine the effect of control inputs on the stability and steering capabilities. The time histories of aileron, horizontal tail, and vertical-tail deflections from this flight are

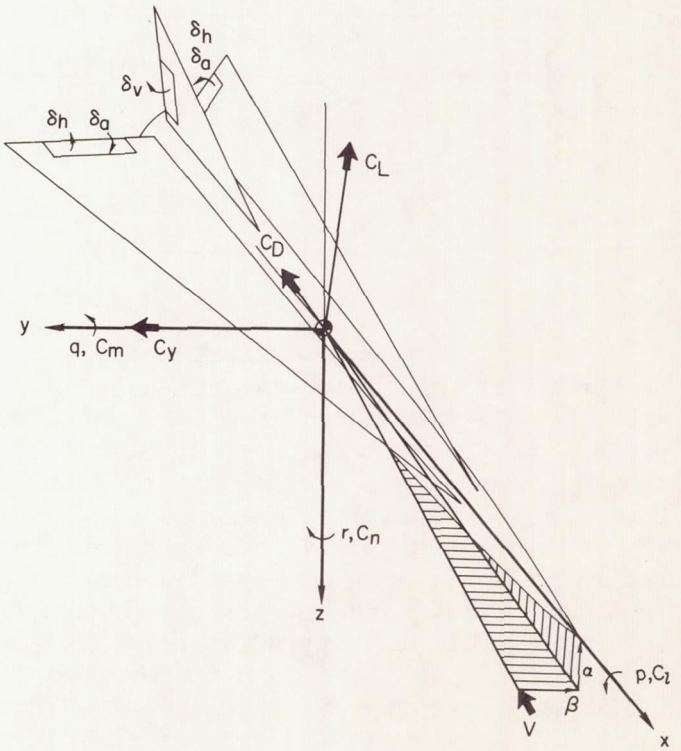

Figure 4.- Positive sense for coordinate system, aerodynamic coefficients, and control deflections. Arrows indicate positive sense.

shown in figure 5. Since the digital program could not accept continuous control changes, it was necessary to approximate the control inputs as shown by the dashed lines in the figure.

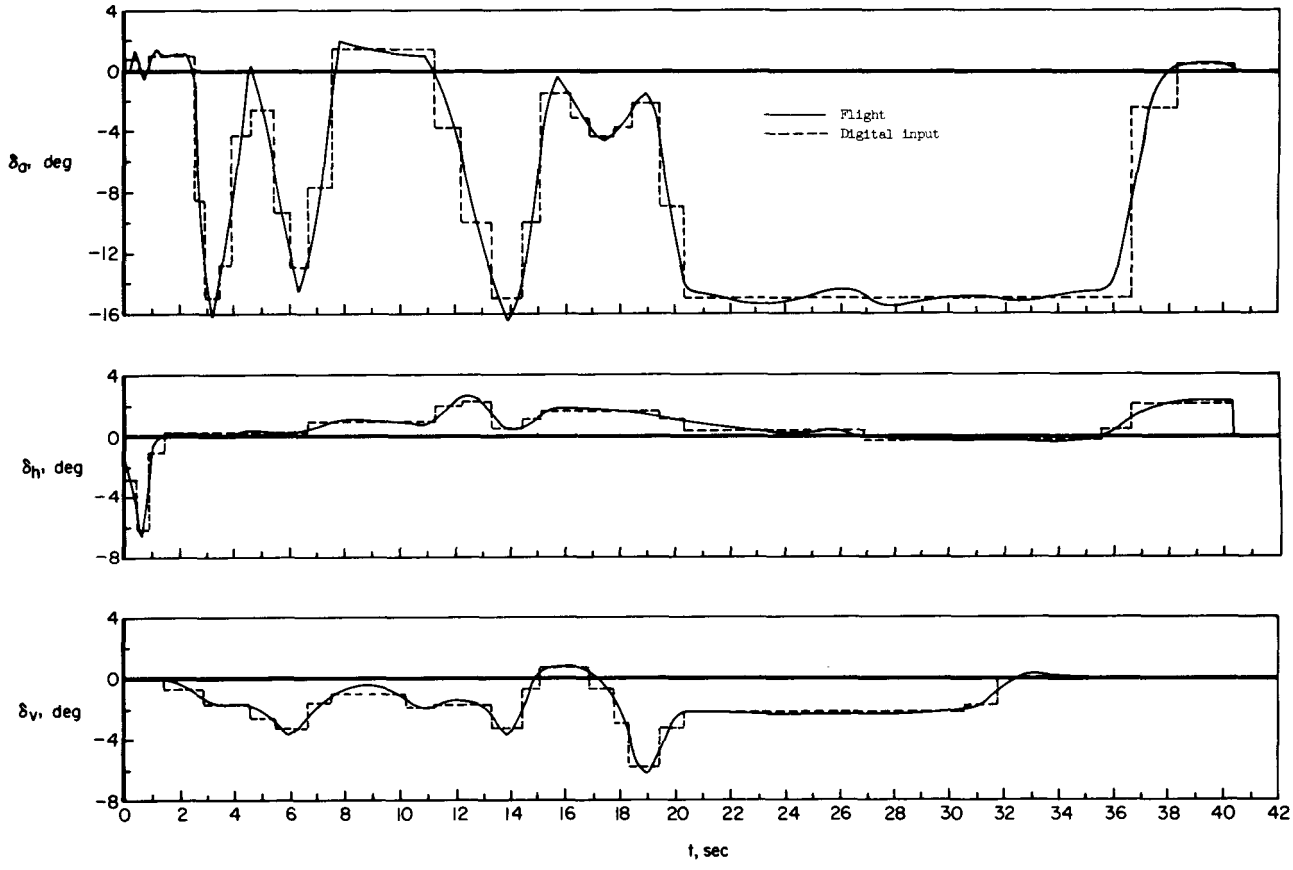

Figure 5.- Time histories of control deflections.

Results of the calculations are compared with the flight data in figure 6 as the variation of lateral displacement from the initial heading at touchdown with the slideout distance. The control inputs given in figure 5 produce the perturbations in the lateral displacement shown in figure 6. The numerals along the curves of figure 6 indicate the time during slideout by which the control inputs and lateral displacements can be correlated. Comparison of the calculated results and flight data indicates that the effects of control inputs on the lateral displacement during slideout can be predicted reasonably well by equations (16). One heading change not predicted by the calculations occurred at an actual slideout time of approximately 20 seconds. However, in figure 5 it can be seen that there were no recorded control inputs to change the heading during this portion of the slideout. This displacement was probably caused by a variation in the lakebed surface on which the X-15 lands.

In addition to the effects of control inputs on slideout, it can be seen from figure 6 that the calculated slideout distance is 6,863 feet, which is 5 percent greater than the actual slideout distance, and the calculated lateral displacement is 117 feet, which is 19 percent less than the actual value. These

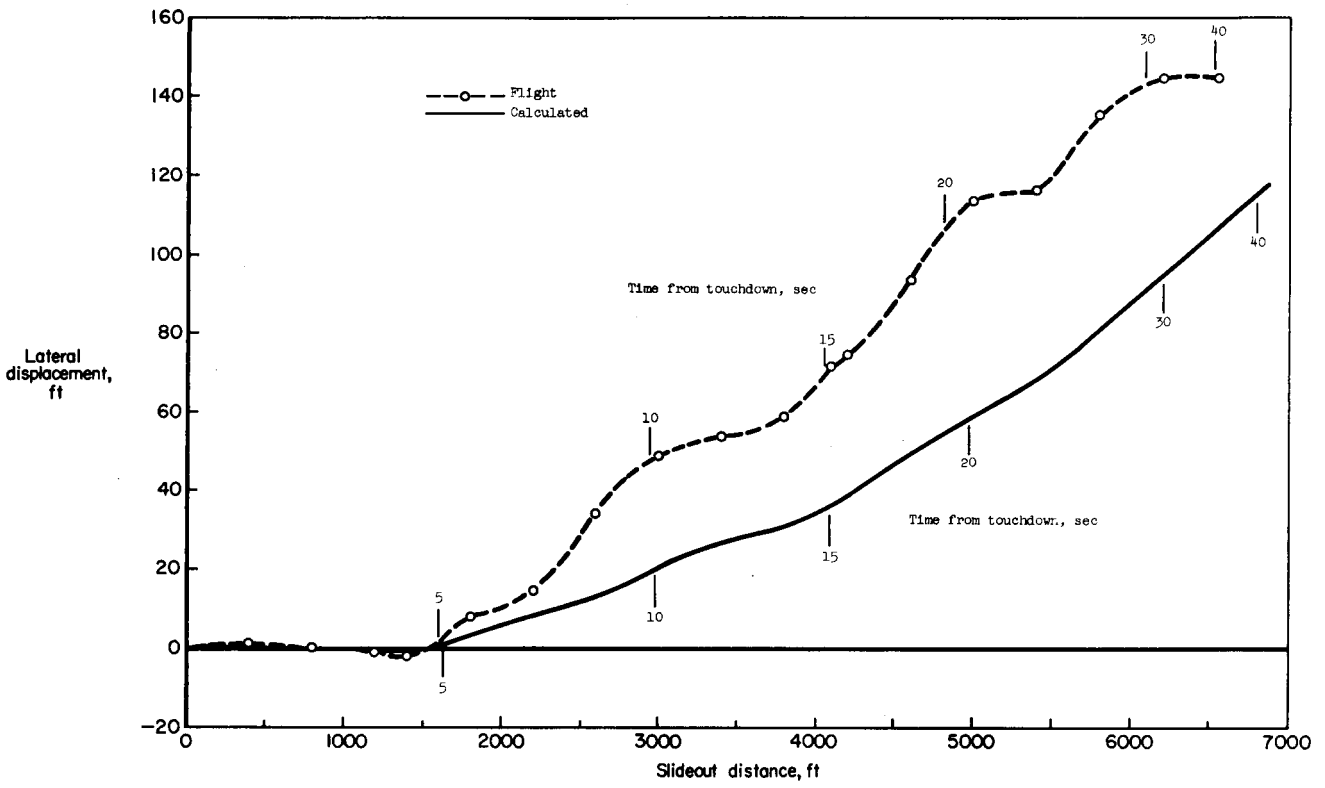

Figure 6.- Variation of lateral displacement with slideout distance.

results show that the three-degree-of-freedom slideout analysis represented by equations (16) adequately predicts the slideout distance, the direction of lateral deviations, and the magnitude of lateral displacement of the vehicle.

Several factors omitted from consideration in the calculations were: variations in the aerodynamic derivatives and the coefficients of friction; the effect of ground plane on the aerodynamic derivatives; the oscillations of the vehicle during the landing impact; and deviations from the initial heading, although no intentional control inputs are made. A detailed study of the influence of these factors on the slideout is beyond the scope of this paper.

The effectiveness of lateral control inputs on the slideout is seen in the lateral displacement which is achieved. The results of a study of the effectiveness for one aileron setting for the X-15 are presented in figure 7. The lateral displacement is shown in the figure as a function of the velocity at which a control is removed during the slideout. The calculations were performed assuming that 15° of aileron control are applied immediately at a touchdown velocity of 200 knots. The abscissa of figure 7, therefore, is the velocity at which the control position is neutralized; that is, the point at zero indicates that the control is not removed during the slideout, whereas the point at 200 knots indicates that the control is removed immediately at touchdown. Figure 7 shows that if the control input is not removed until the vehicle has decelerated to about 100 knots, there is negligible effect on the lateral displacement; however, if the control is removed immediately after touchdown, or before the vehicle has

decelerated to about 100 knots, the effect on the lateral displacement is significant. These results indicate that the effect of control inputs is greatest between the touchdown velocity and 100 knots. Thus, the aerodynamic influence on the vehicle as indicated by the control effectiveness becomes negligible at about 100 knots.

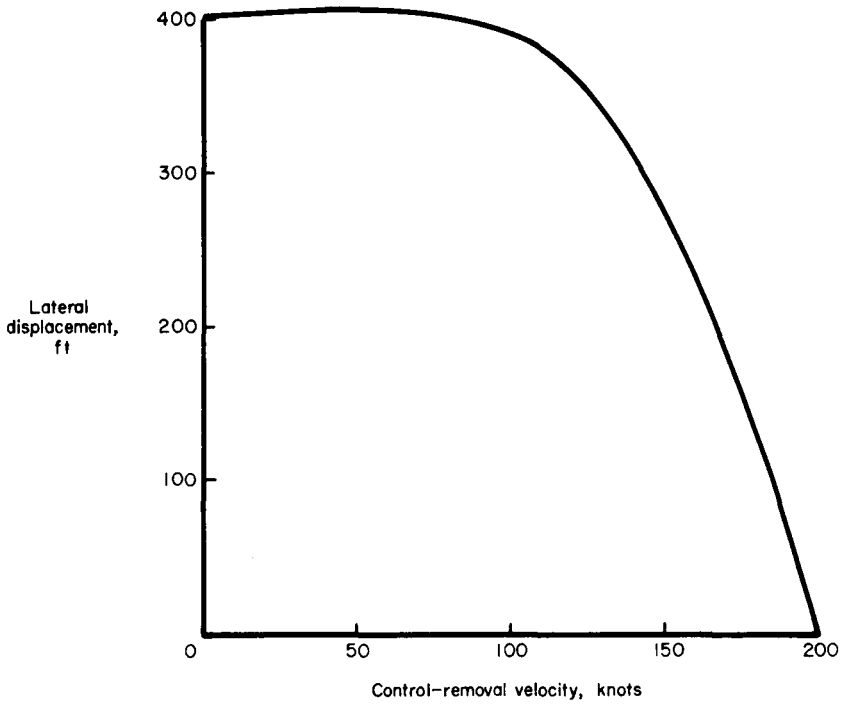

Figure 7.- Lateral displacement as a function of the velocity at which an aileron deflection of 15° is removed.

CONCLUDING REMARKS

A theoretical analysis has been presented for the slideout dynamics of a vehicle equipped with a tricycle skid-type landing-gear system. The general slideout equations were reduced to three degrees of freedom, and calculations were made with these equations in order to compare the theoretical slideout with flight-test data and to study the effectiveness of aerodynamic controls on the lateral displacement during slideout.

The results of the investigations indicate that the three-degree-of-freedom equations adequately predict slideout distance, the direction of lateral displacement, the approximate lateral displacement, and the velocity at which the aerodynamic influence on the vehicle becomes negligible.

Flight Research Center,
National Aeronautics and Space Administration,
Edwards, Calif., March 1, 1963.

APPENDIX A

DETERMINATION OF LANDING-GEAR DEFLECTION

The vertical distances from the ground plane of the center of gravity and of the point of attachment of the main gear to the fuselage are related to the vehicle geometry as shown in figure 1. Analysis of the right main gear yields

$$z_o = h_2' + \left(d \cos \varphi + S_2 \sin \varphi\right)\cos \theta + L_{HM} \sin \theta \tag{A1}$$

where

$$h_2' = h_2 \cos \theta$$

Since the rate of change of height of the main gear point of attachment with respect to the ground is equal to the rate of gear vertical deflection, that is,

$$\dot{h}_2' = \dot{\delta}_{M_2} \tag{A2}$$

the following relation is valid:

$$\dot{\delta}_{M_2} = \dot{z}_o - \left[L_{HM} \cos \theta - \left(d \cos \varphi + S_2 \sin \varphi\right)\sin \theta\right]\dot{\theta} - \left(S_2 \cos \varphi - d \sin \varphi\right)\dot{\varphi} \cos \theta \tag{A3}$$

The rate of vertical deflection for the left main gear is:

$$\dot{\delta}_{M_1} = \dot{z}_o - \left[L_{HM} \cos \theta - \left(d \cos \varphi - S_1 \sin \varphi\right)\sin \theta\right]\dot{\theta} + \left(S_1 \cos \varphi + d \sin \varphi\right)\dot{\varphi} \cos \theta \tag{A4}$$

APPENDIX B

TRIGONOMETRIC RELATIONS FOR THE ANGLE λ

The angle in the ground plane between the x_o-axis and the friction force on a skid is denoted by λ_i where the subscript i indicates the skid being considered (see fig. 1). The friction force on each skid will be in a direction parallel and opposite to the direction of the velocity of the skid relative to the ground. If the magnitude of the skid velocity is known, it is possible to determine the trigonometric relations for the λ_i angles.

The relative velocity of any position on a vehicle as measured in the ground plane is expressed as:

$$\left(V_G\right)_i^2 = \left(V'_{x_o}\right)_i^2 + \left(V'_{y_o}\right)_i^2 \tag{B1}$$

The ground velocity components V'_{x_o} and V'_{y_o} are related to body axes by

$$\left.\begin{aligned} \left(V'_{x_o}\right)_i &= V'_{x_i} \cos\theta + \left(V'_{y_i} \sin\varphi + V'_{z_i} \cos\varphi\right)\sin\theta \\ \left(V'_{y_o}\right)_i &= V'_{y_i} \cos\varphi - V'_{z_i} \sin\varphi \end{aligned}\right\} \tag{B2}$$

where

$$\left.\begin{aligned} V'_{x_i} &= u' + qz_i - ry_i \\ V'_{y_i} &= v' + rx_i - pz_i \\ V'_{z_i} &= w' + py_i - qx_i \end{aligned}\right\} \tag{B3}$$

The components of the relative velocity of the center of gravity are denoted by the primed quantities. In order to determine these velocities, it is first necessary to investigate the relationship of the vehicle relative velocity, center-of-gravity relative velocity, and wind velocity, which is

$$\overline{V} = \overline{V}' + \overline{V}_w \tag{B4}$$

where

$\bar{V}$ is the velocity vector of the vehicle center of gravity relative to the airstream

$\bar{V}'$ is the velocity vector of the vehicle center of gravity relative to the ground

$\bar{V}_w$ is the velocity vector of the wind relative to the ground

Assume that a wind of constant velocity V_w is blowing at a constant angle ψ_w to the initial heading X and parallel to the ground plane. Then, the wind components in the fixed-earth system are:

$$\left.\begin{aligned} u_{w_o} &= V_w \cos \psi_w \\ v_{w_o} &= V_w \sin \psi_w \end{aligned}\right\} \quad (B5)$$

Transformation of these velocities to body coordinates (see fig. 2) yields:

$$\left.\begin{aligned} u_w &= \left(u_{w_o} \cos \psi + v_{w_o} \sin \psi\right)\cos \theta \\ v_w &= \left(v_{w_o} \cos \psi - u_{w_o} \sin \psi\right)\cos \varphi + \left(u_{w_o} \cos \psi + v_{w_o} \sin \psi\right)\sin \theta \sin \varphi \\ w_w &= \left(u_{w_o} \cos \psi + v_{w_o} \sin \psi\right)\sin \theta \cos \varphi - \left(v_{w_o} \cos \psi - u_{w_o} \sin \psi\right)\sin \varphi \end{aligned}\right\} \quad (B6)$$

The components of wind velocity given by equations (B6) and the components of $\bar{V}$ given by equations (8) are used in equation (B4) to determine the primed velocities as follows:

$$\left.\begin{aligned} u' &= \left[V \cos \beta - V_w\left(\cos \psi_w \cos \psi + \sin \psi_w \sin \psi\right)\right]\cos \theta \\ v' &= V \sin \beta - V_w \left[\left(\sin \psi_w \cos \psi - \cos \psi_w \sin \psi\right)\cos \varphi \right. \\ &\quad \left. + \left(\cos \psi_w \cos \psi + \sin \psi_w \sin \psi\right)\sin \theta \sin \varphi\right] \\ w' &= V \cos \beta \sin \theta - V_w\left[\left(\cos \psi_w \cos \psi + \sin \psi_w \sin \psi\right)\sin \theta \cos \varphi \right. \\ &\quad \left. - \left(\sin \psi_w \cos \psi - \cos \psi_w \sin \psi\right)\sin \varphi\right] \end{aligned}\right\} \quad (B7)$$

The velocities given by equations (B1) and (B2) are used to determine the trigonometric relations for λ_i, which are:

$$\left.\begin{aligned} \cos \lambda_i &= \frac{\left(V'_{x_o}\right)_i}{\left(V_G\right)_i} \\ \sin \lambda_i &= \frac{\left(V'_{y_o}\right)}{\left(V_G\right)_i} \end{aligned}\right\} \quad (B8)$$

For the slideout of the vehicle represented by equations (15), the velocity relations given by equations (B2) become:

$$\left.\begin{aligned} \left(V'_{x_o}\right)_i &= V \cos \beta - \dot{\psi} y_i - V_w\left(\cos \psi_w \cos \psi + \sin \psi_w \sin \psi\right) \\ \left(V'_{y_o}\right)_i &= V \sin \beta + \dot{\psi}\left(x_i \cos \theta + z_i \sin \theta\right) - V_w\left(\sin \psi_w \cos \psi - \cos \psi_w \sin \psi\right) \end{aligned}\right\} \quad (B9)$$

For the slideout of a vehicle in low pitch attitude, equations (B2) become:

$$\left.\begin{aligned} \left(V'_{x_o}\right)_i &= V \cos \beta - \dot{\psi} y_i - V_w\left(\cos \psi_w \cos \psi + \sin \psi_w \sin \psi\right) \\ \left(V'_{y_o}\right)_i &= V \sin \beta + \dot{\psi} x_i - V_w\left(\sin \psi_w \cos \psi - \cos \psi_w \sin \psi\right) \end{aligned}\right\} \quad (B10)$$

APPENDIX C

INITIAL CONDITIONS AND CALCULATIONS OF EULER YAW ANGLE, SLIDEOUT DISTANCE, AND LATERAL DISTANCE

The first derivative of V, β, and r with respect to time can be written in the form of the parabolic-difference equations of reference 14 as

$$\left.\begin{aligned} V_{n+1} &= 2\epsilon\dot{V}_n + V_{n-1} \\ \beta_{n+1} &= 2\epsilon\dot{\beta}_n + \beta_{n-1} \\ r_{n+1} &= 2\epsilon\dot{r}_n + r_{n-1} \end{aligned}\right\} \qquad (C1)$$

where

ϵ is the length of the time increment

n is the time interval being considered

By designating the touchdown increment by $n = 0$, the conditions immediately after touchdown are dependent upon the conditions prior to and at touchdown. The conditions at touchdown are selected arbitrarily. It is assumed for the numerical example that the vehicle has a sideslip angle due only to a deviation in wind direction from the vehicle's initial heading and that the vehicle has no initial rotational rates. It is further assumed that these conditions hold immediately prior to touchdown. These conditions, together with the velocity initial condition, are expressed as:

$$\left.\begin{aligned} V_0 &= V_{\text{touchdown}} \\ \beta_0 &= \beta_{-1} \approx \psi_w \\ r_0 &= r_{-1} = 0 \end{aligned}\right\} \qquad (C2)$$

It is also assumed that the vehicle is decelerating linearly from a time prior to touchdown to a time after touchdown. Then V_{-1} becomes:

$$V_{-1} = 2V_0 - V_1 \qquad (C3)$$

The equations for the Euler yaw angle, slideout distance, and lateral distance from initial heading, obtained by the use of the trapezoidal-difference techniques of reference 14 are:

$$\left.\begin{aligned}
\psi_{n+1} &= \psi_n + \frac{\epsilon}{2}\left(r_{n+1} + r_n\right) \\
X_{n+1} &= X_n + \frac{\epsilon}{2}\left[V_{G_n} \cos\left(\psi_n + \beta'_n\right) + V_{G_{n+1}} \cos\left(\psi_{n+1} + \beta'_{n+1}\right)\right] \\
Y_{n+1} &= Y_n + \frac{\epsilon}{2}\left[V_{G_n} \sin\left(\psi_n + \beta'_n\right) + V_{G_{n+1}} \sin\left(\psi_{n+1} + \beta'_{n+1}\right)\right]
\end{aligned}\right\} \quad (C4)$$

The angle β' is measured in the ground plane between the x_o-axis and the relative velocity of the center of gravity in the ground plane. The angle is determined by

$$\beta'_n = \sin^{-1}\left(\frac{V'_{y_{o_n}}}{V_{G_n}}\right) \quad (C5)$$

where referring to equations (12), (B2), and (B3),

$$\left.\begin{aligned}
V'_{x_{o_n}} &= u' \cos\theta + w' \sin\theta \\
V'_{y_{o_n}} &= v'
\end{aligned}\right\} \quad (C6)$$

and V_{G_n} is given by equation (B1).

REFERENCES

1. Zalovcik, John A.: Calculated Effect of Some Airplane Handling Techniques on the Ground-Run Distance in Landing on Slippery Runways. NACA TN 4058, 1957.

2. Zalovcik, John A.: Ground Deceleration and Stopping of Large Aircraft. AGARD Rep. 231, 1958.

3. Scherberg, Max G., and Tifford, Arthur: Shortening Landing Ground Roll by Roll Attitude. WADC Tech. Rep. 57-16 (ASTIA Doc. No. AD118020), Wright Air Dev. Center, U. S. Air Force, Jan. 1957.

4. Marquard, E.: Schwingungsdynamik des Schnellen Strassenfahrzeugs (Vibration Dynamics of the Fast Road-Vehicle). Girardet Vereag (Essen, Germ.), 1952, ch. 12. (Eng. translation available from Smuts Tech. Services, 12 Thorndene Ave., London, N. 11, Eng.)

5. Fisher, Lloyd J., Jr.: Landing Energy Dissipation for Manned Reentry Vehicles. NASA TN D-453, 1960.

6. Fisher, Lloyd J., Jr.: Landing-Impact-Dissipation Systems. NASA TN D-975, 1961.

7. Houbolt, John C., and Batterson, Sidney A.: Some Landing Studies Pertinent to Glider-Reentry Vehicles. NASA TN D-448, 1960.

8. McKay, James M., and Scott, Betty J.: Landing-Gear Behavior During Touchdown and Runout for 17 Landings of the X-15 Research Airplane. NASA TM X-518, 1961.

9. Blanchard, Ulysse J.: Landing Characteristics of a Winged Reentry Vehicle With All-Skid Landing Gear Having Yielding-Metal Shock Absorbers. NASA TN D-1496, 1962.

10. Wolowicz, Chester H., and Holleman, Euclid C.: Stability-Derivative Determination From Flight Data. AGARD Rep. 224, 1958.

11. Dreher, Robert C., and Batterson, Sidney A.: Coefficients of Friction and Wear Characteristics for Skids Made of Various Metals on Concrete, Asphalt, and Lakebed Surfaces. NASA TN D-999, 1962.

12. Kolk, Richard W.: Modern Flight Dynamics. Prentice-Hall, Inc., 1961, ch. 2.

13. Etkin, Bernard: Dynamics of Flight – Stability and Control. John Wiley & Sons, Inc., 1959, ch. 4.

14. Milne, William Edmund: Numerical Solution of Differential Equations. John Wiley & Sons, Inc., 1953, ch. 2.